



Flue gas injection for EOR and sequestration: Case study



Serdar Bender^{a,*}, Serhat Akin^b

^a Turkish Petroleum, 06530, Ankara, Turkey

^b Middle East Technical University, 06800, Ankara, Turkey

ARTICLE INFO

Keywords:

CO₂
Flue gas
Simulation
EOR
Sequestration
Mature

ABSTRACT

The combination of carbon dioxide enhanced oil recovery (CO₂-EOR) and permanent CO₂ storage in mature oil reservoirs has the potential to provide a critical near-term solution for reducing greenhouse gas (GHG) emissions. This solution involves the combined application of carbon capture and storage from power generation and other industrial facilities with CO₂-EOR. In order to reduce CO₂ capture costs flue gas, which consists mainly of N₂ and CO₂, injection has been proposed. The main aim of this research is to investigate flue gas injection in a mature oil field located in Turkey where CO₂ EOR had been applied between 2003 and 2012. Injected CO₂ was produced from a nearby small natural CO₂ reservoir with limited resource. Due to the availability of nearby flue gas source (cement factory) and a pipeline for gas transportation, which was built to transport natural gas from the oil field to cement factory, there is a huge opportunity to decrease project costs. A 3D compositional simulation model was built after a detailed fluid characterization. After history matching 31 years of production, injection, saturation and pressure history, a comparative study was conducted to examine the efficiency of flue gas injection compared to CO₂ injection for simultaneous EOR and storage purposes. Storage capacity of the oil field as well as the contribution of raw flue gas injection and CO₂ injection to oil recovery were studied. Effect of injected gas type, gas solubility and operating parameters on storage and recovery were investigated. Results showed that pure CO₂ injection leads to higher oil recovery and CO₂ storage, if injection continued for at least 25 years. Before this threshold injection time, flue gas injection and pure CO₂ injection resulted in comparable oil recoveries. It was also concluded that pressurizing the reservoir with raw flue gas injection followed by pure CO₂ injection may improve the project economics.

1. Introduction

One of the major sources of anthropogenic greenhouse gases is cement industry. An average of 5% of the CO₂ emissions is due to cement industry (Arachchige et al., 2013). Flue gas containing high amount of CO₂ is emitted during cement clinker production and during fuel combustion. Composition of the flue gas depends on the fuel used for combustion process, but it mainly consists of N₂, CO₂, water vapor, O₂ and SO₂. Sulfur, NO_x, CO, CO₂ and dust are some of the air polluting components that may be present in flue gases (Testo, 2004).

CO₂ and non-CO₂ emissions produced as flue gas during cement production can be sequestered in underground geologic formations such as coal seams, mature or depleted hydrocarbon reservoirs and

deep saline aquifers (Bender, 2011). There are four basic mechanisms that required for long term successful geologic CO₂ storage: stratigraphic/structural, residual, solubility and mineral trapping (Zhang and Song, 2014). If there is a good seal, CO₂ will be trapped permanently and will be immobile with the contribution of these mechanisms (Kovscek, 2002). There are many studies in the literature that discuss CO₂ storage and CO₂ EOR (Wickramathilaka and Willis, 2011; Shaw and Bachu, 2002; Jessen and Stenby, 2007; Eide et al., 2015; Beckwith, 2011; Pike, 2006; Reichl et al., 2015; Rao and Hughes, 2011); however, only a few studies have been made on flue gas injection (Koch and Hutchinson, 1958; Fong et al., 1992; Huang, 1997; Zhang et al., 2006; Shokoya et al., 2005; Rivera de la Ossa et al., 2010; Trevisan et al., 2013; Dong and Huang, 2002; Fong et al., 1992). Majority of these studies was focused on maximizing

* Corresponding author.

E-mail address: sbender@tp.gov.tr (S. Bender).

Table 1
Flue gas stream, composition and properties used for simulation.

Factory Operating Level	Low	Medium	High
CO ₂ , %	24.5	24.5	24.5
N ₂ , %	75.5	75.5	75.5
Mass Flow,CO ₂ , kg/hr	45,637	68,456	91,275
Mass Flow,N ₂ , kg/hr	88,409	132,613	176,818

the oil recovery not flue gas storage. Injecting raw flue gas into oil reservoirs is very attractive because these reservoirs have structural seals for trapping that are well studied and characterized. These fields have surface facilities and wells which will also decrease the capital investments of the storage project. Injecting flue gas into producing oil fields may result in incremental oil recovery and make the storage project more feasible. Availability of the flue gas source has

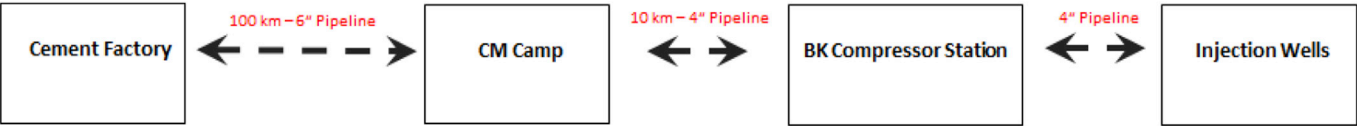


Fig. 1. Cement factory to injection wells pipeline schematic.

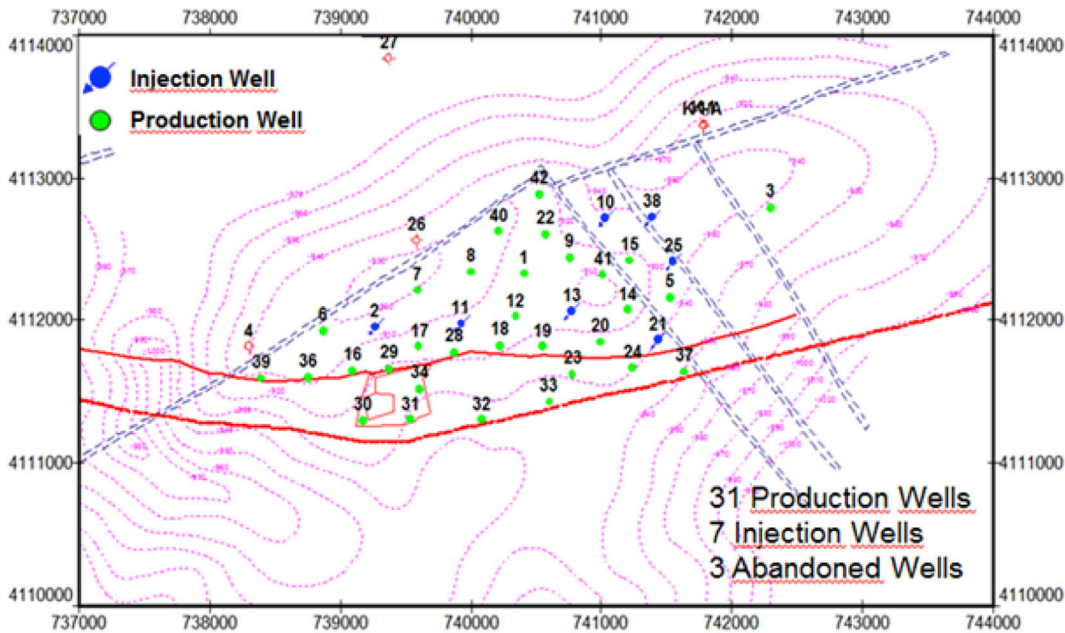


Fig. 2. Field structure map.

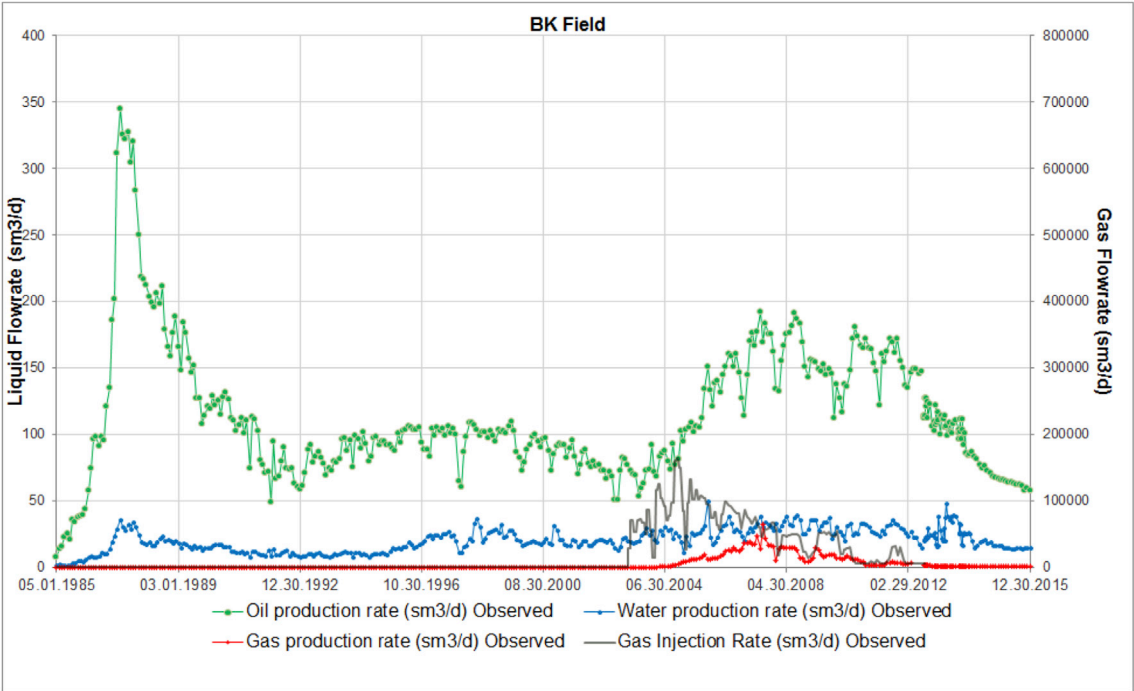


Fig. 3. Field production & injection history.

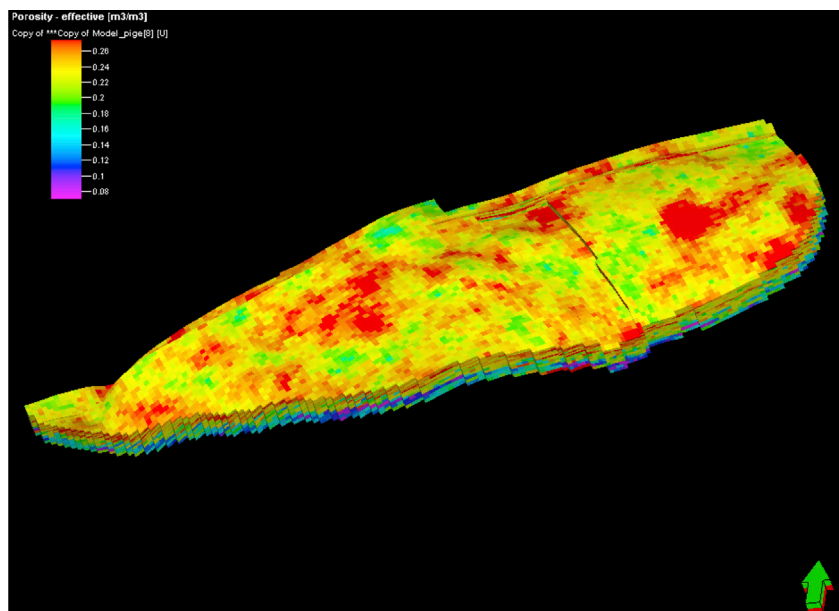


Fig. 4. Porosity distribution map.

strong effect on project economics.

In this study, flue gas storage capacity of a CO₂ flooded oil reservoir was determined. It was assumed that injected flue gas was transported from a nearby cement factory by using available pipelines and injected by deriving benefit from facilities that were pre-used for CO₂ flooding project. Contribution of raw flue gas injection to oil recovery was examined by conducting compositional numerical simulation. A comparative study was conducted to investigate the efficiency of flue gas injection compared to CO₂ injection for simultaneous EOR and storage. Effect of injected gas types, CO₂ solubility, and operating strategies on storage and recovery were studied.

2. Case study

2.1. Flue gas source

Emissions related with cement industry can be divided into two groups; CO₂ emissions and others. CO₂ emissions occur during the

process of calcination (Eq. (1)) and also occur during energy production. Majority of the CO₂ (50%) is released during calcination. This is followed by fossil fuel combustion (40%), transportation (5%) and electricity consumption (5%) (Mahasen et al., 2005). Average CO₂ released during the production of portland cement in USA is 0.927 kg of CO₂ per 1 kg of cement (Marceau et al., 2006). Gross CO₂ emissions factor for China's cement sector is 0.883 kg of CO₂ per 1 kg of cement where 0.415 kg comes from calcination and 0.467 kg comes from energy production (Shen et al., 2014). CO₂ is not the only greenhouse gas emitted to atmosphere during cement production. SO_x, NO_x, CO, N₂, O₂ and volatile organic compounds and dust may also be released during cement production. Among these CO₂, NO_x, SO_x, CO and some of the volatile organic compounds are greenhouse gases. Amount of these emissions is based on cement type, cement production method and type of fuels used for the process. Flue gas composition used in this study (Table 1) is taken from (Nazmul, 2005). It is assumed that NO_x, SO₂, O₂ and H₂O are removed from the flue gas before injecting into reservoir.

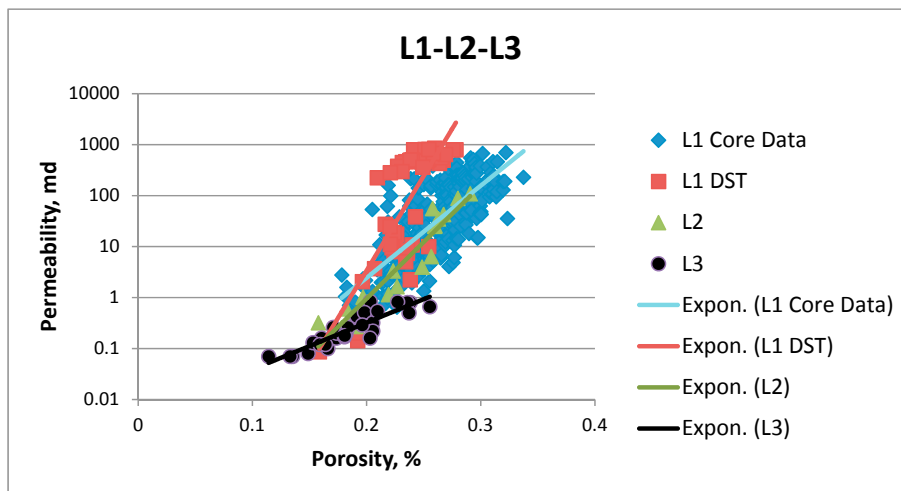


Fig. 5. Permeability & porosity relationship for Layer-1, Layer-2, and Layer-3.

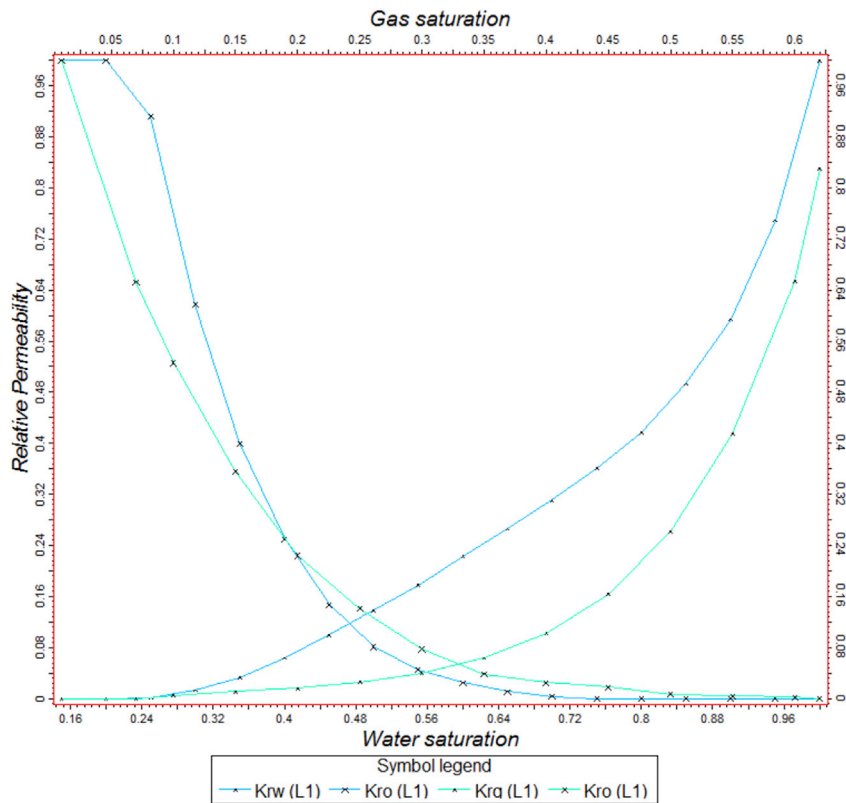


Fig. 6. Relative Permeability vs. Water & Gas Saturation for Layer-1.

$\text{CaCO}_3 + \text{heat} \leftrightarrow \text{CaO} + \text{CO}_2$ (1)

Cement factory whose flue gas is to be used is located in Turkey

close to heavy oil field where the injection will be carried out. Cement production has been started in 1975. Factory was reconstituted in 1980 to operate with natural gas and coal as an alternative fuel to oil due increasing oil prices (Mardin Cement, 2015). Natural gas had been

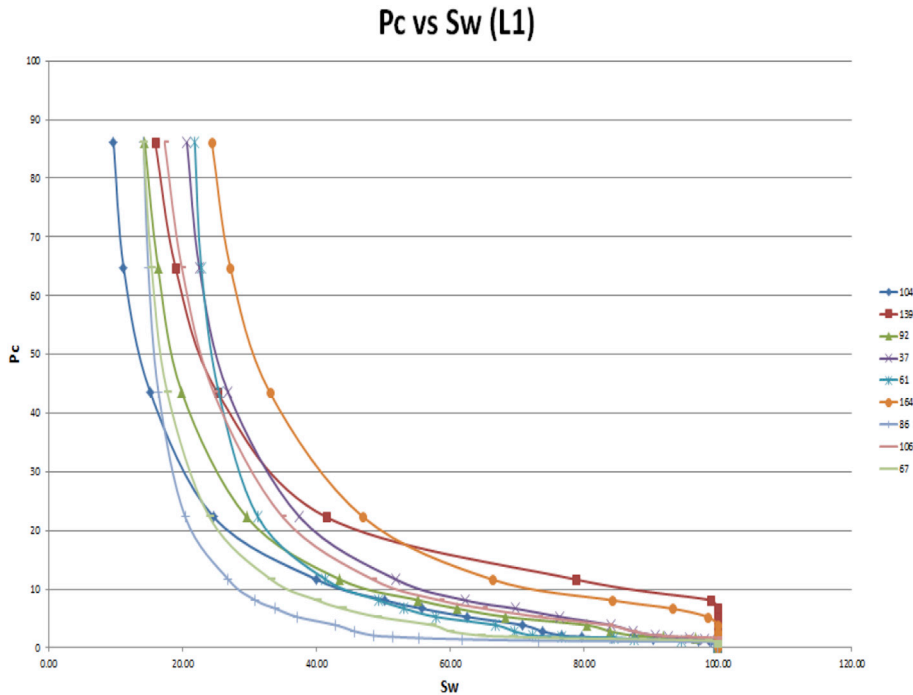


Fig. 7. Capillary Pressure vs. Water Saturation for Layer-1.

Table 2
Molar compositions of oil.

Component	Mol, %	Component	Mol, %	Component	Mol, %
H2S	0.00001	C10	13.359	C24	0.45
CO ₂	0.0003	C11	10.36	C25	0.12
N2	0.0001	C12	5.67	C26	0.27
CH4	1.0021	C13	5.94	C27	1.83
C2	1.33	C14	4.82	C28	1.33
C3	1.66	C15	5.74	C29	0.87
nC4	2.54	C16	1.57	C30	0.14
iC4	0.67	C17	2.22	C31	0.36
nC5	0.05	C18	2.3	C32	0.31
iC5	0.02	C19	0.28	C33	0.28
C6	2.479	C20	0.61	C34	0.23
C7	3.7506	C21	1.11	C35	0.22
C8	11.71	C22	0.67	C36 +	0.3
C9	12.69	C23	0.74	–	–

supplied between 1982 and 2012 from a nearby gas field. CM is the main camp where all the production from nearby fields was gathered. To transport the natural gas from CM camp to cement factory, 100 km long and 6" diameter pipeline was constructed (Fig. 1). In this study, the idea is to use the same pipeline for flue gas transportation to reduce the project costs. Instead of transporting natural gas from the camp to factory, flue gas will be transported from cement factory to camp and then to compressor station. Pipeline between CM camp and compressor station is 10 km long and has a 4" diameter. Since measured CO₂ emission data from the factory is not available, clinker

Table 3
Summary of the reservoir model properties.

Parameters	Values	Units
Number of cells in the x direction	152	
Number of cells in the y direction	54	
Number of cells in the z direction	13	
Number of gridblocks	106,704	
x gridblock size	50	m
y gridblock size	50	m
z gridblock size	3–5	m
Total pore volume	1.62E+08	Rm ³

production data was used to calculate the amount of gas emissions. Using average clinker production (2400 tons of clinker per day) and IPCC default value of fraction of lime in clinker (64.6%) (Gibbs et al., 2001), clinker emission factor was calculated as 0.507 tons of CO₂ per tons of clinker by using Eq. (2). As a result, CO₂ emission was calculated as 1217 tons/day from calcining process and CO₂ emission from fuel combustion was calculated as 973.6 tons/day. Total gas flow rates are given in Table 1 for different operating levels of the cement factory.

$$EF_{\text{clinker}} = \text{fraction CaO} \times (44.01 \text{ g/mole CO}_2 / 56.08 \text{ g/mole CaO}) \quad (2)$$

2.2. Field development

The heavy oil carbonate reservoir was discovered in 1985 (Bender

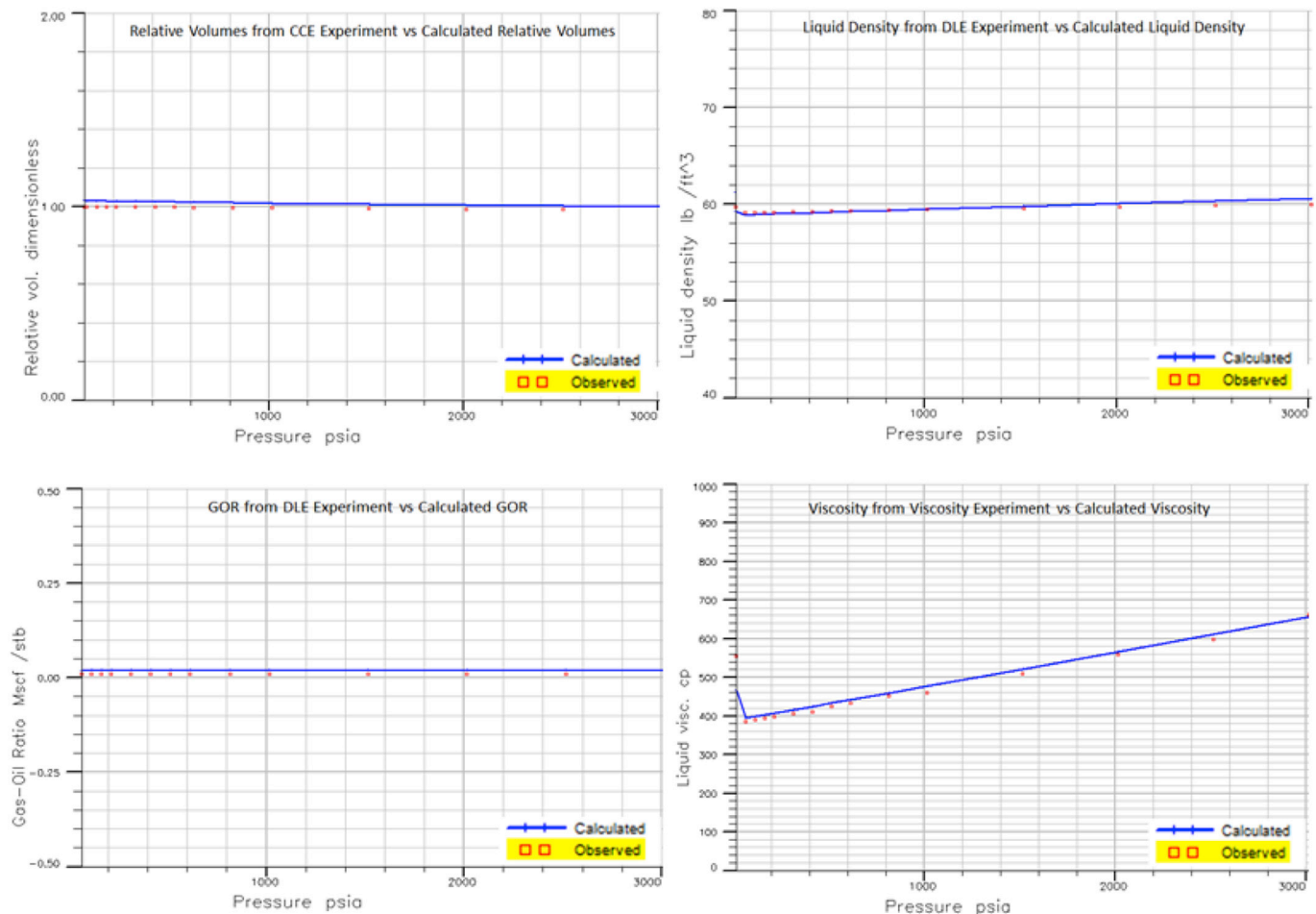


Fig. 8. Laboratory Observed Data vs Simulation Results.

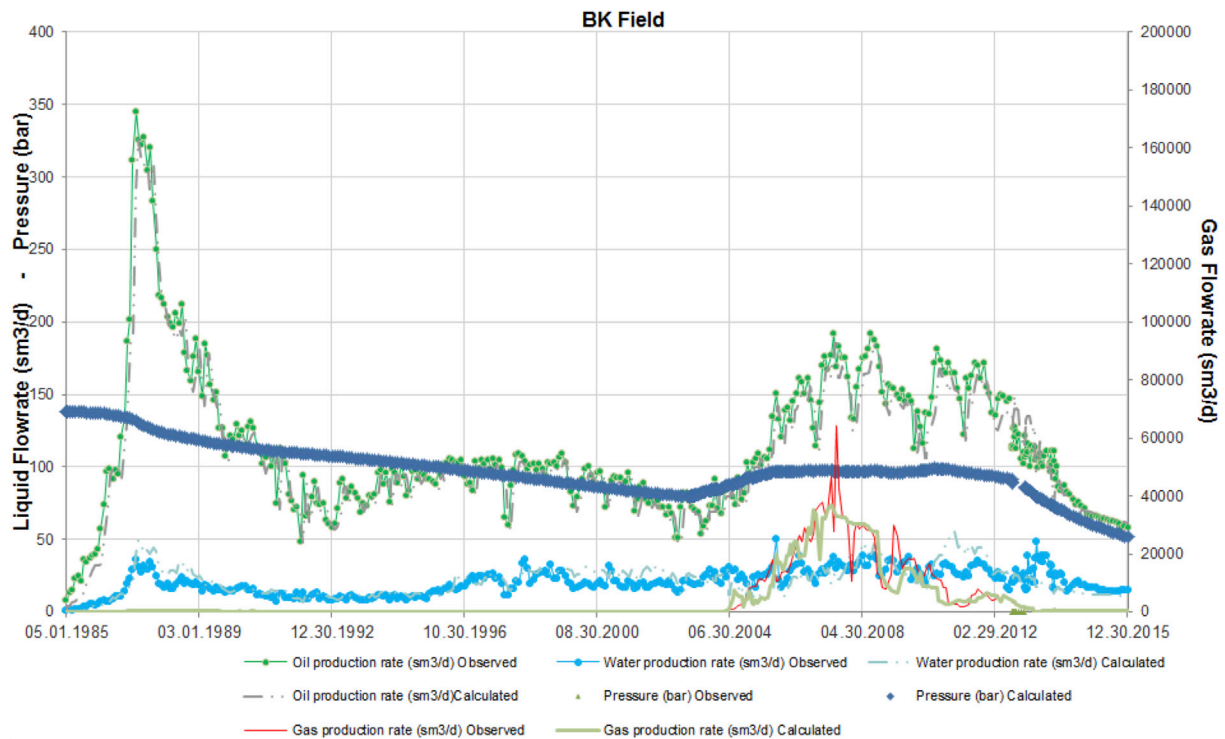


Fig. 9. History match of the field oil-water-gas production rate, and pressure.

and Yilmaz, 2014). The reservoir began primary production in 1985 and developed with 41 wells (Fig. 2). Peak daily oil production reached to 300 m^3/day in 1987 (Fig. 3); however, there was a sharp decline after 1987 due to lack of pressure support, low voidage displacement, low API and high oil viscosity. Production plateau period had started in 1994 and continued until 2002. Continuous CO_2 injection was started in May 2003 by 7 injection wells. The effect of the CO_2 injection on oil production was seen after 12 months of injection period corresponding to breakthrough time of CO_2 . It had been observed that oil production increased and water production decreased in the field. Due to high gas oil ratios in the production wells and low sweep efficiencies, water alternating gas injection had been started in 2007 that doubled the daily oil production (Fig. 3). More than 240 Msm^3 of additional oil was produced by CO_2 injection with 900 sm^3/sm^3 CO_2 oil ratio. However, after stopping the CO_2 injection in 2012 due to depletion of CO_2 reservoir, decline in oil production has started again and today daily oil production decreased to half of the project time's production.

2.3. Model development

2.3.1. Geologic description

The heavy oil field is located in a tectonically active area in Turkey dominated by WSW-ENE oriented faults, anticlinal features and southerly formation dips (Bender and Yilmaz, 2014). The reservoir is bounded by a sealing normal fault at the north. Crest of the asymmetric anticline dipping towards the south leant to this normal fault. There are three major partially sealing NW-SE oriented strike slip faults (Fig. 2). Main production formation is Alt Sinan Formation with an average thickness of 60 m. From core and log studies, it was understood that there are three facies in the reservoir. In the simulation study, these facies were represented by three different layers. Bottom layer has 10–18% of porosity bearing wackestone with very low permeability. Second layer has 15–20% of porosity bearing packstone with low permeability

(Cobanoğlu, 2001). Top layer has 22–30% of porosity bearing grainstone with the highest permeability where main production is taking place. Thickness of the first layer increases from west to east of the field and thicknesses of the second and the bottom layers decrease from west to east.

2.3.2. Rock & fluid properties

By using well logs and core data, porosity and permeability distributions were determined. Porosity was computed from neutron-density logs and gamma ray-sonic logs where available. As a result porosity distribution map shown in Fig. 4 is obtained. Based on the analysis of all core data, a relationship was established between porosity and permeability for each layer (Fig. 5). Available special core analysis tests were used to construct relative permeability curves representing oil-water and gas-oil system (Fig. 6). Capillary pressure and relative permeability measurements were used together to calculate the irreducible water saturation and residual oil saturations. Leverett J-function was used to combine all capillary pressure measurements obtained from cores (Fig. 7). Initial water saturation for each grid cell was calculated by using the constructed J-function. Similar plots were developed for layer 2 and 3.

Oil gravity is 12 $^\circ\text{API}$ with a very high viscosity of 480 cp at reservoir conditions. PVT reports and routine API measurements show that there is no areal and vertical change in API gravities in the field (Bender and Yilmaz, 2014). Bubble point pressure is around 50 psia and oil formation volume factor at reservoir conditions is 1.03 rm^3/sm^3 . Solution gas oil ratio is 1.8 sm^3/sm^3 at initial reservoir conditions.

2.3.3. Fluid characterization and component lumping for compositional simulation

Compositional simulation requires an equation of state model (EOS) that describes the relationship between pressure, volume and temperature of a gas or liquid. Molar composition of produced oil given in Table 2 was used in ECLIPSE PVTI. Characterization of heavy plus components

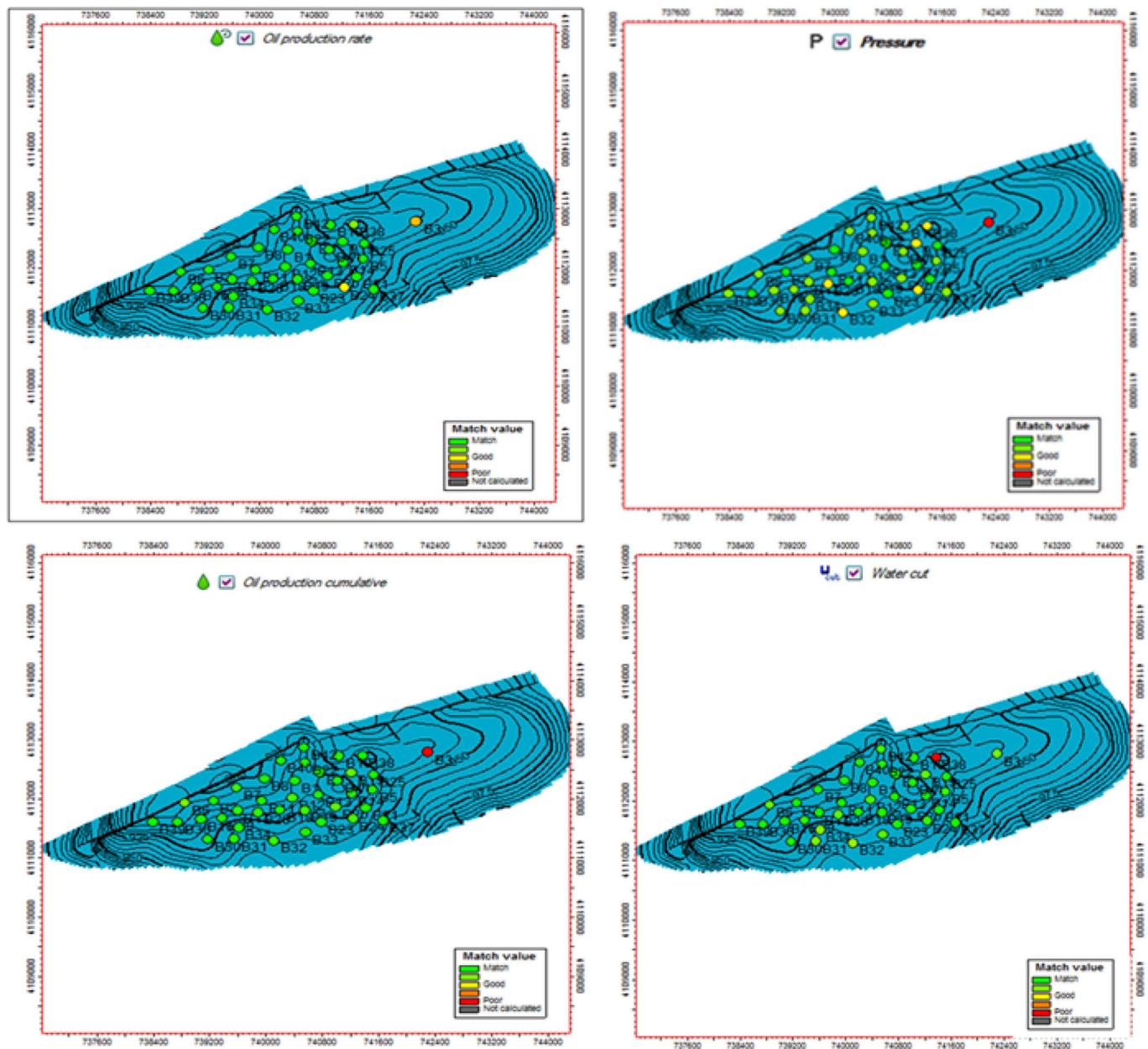


Fig. 10. History match analysis of oil production rate, oil production cumulative, water cut & pressure.

was conducted by using their corresponding molecular weight. Three parameter Peng Robinson EOS, which is a modified version of Soave-Redlich-Kwong EOS was used to calculate the phase behavior (Peng and Robinson, 1976).

To appropriately simulate the flue gas flooding project, CO₂, N₂, and CH₄ gasses were used as pure components. It is quite common to lump C₂-C₃ and C₄-C₆ based on their similar molecular weights (Khan et al., 1992). For C₇ two pseudo components and Whitson's method was used to decide the groups (Whitson, 1983). Components between C₇ and C₁₅ were grouped together and C₁₆ to C₃₆ grouped together. Accuracy of the grouping process was checked by looking the phase diagrams before and after lumping. Created lumping scheme was tuned by acentric factor of C₁₈ (Al-Meshari and McCain, 2005) by matching saturation pressure. Following that, volume shift parameters of all components were used for the regression of the volumetric data of CCE and DLE. Volume shift parameters were also tuned to match liquid density. Finally, viscosity was matched by tuning Zcrit. Fig. 8

presents comparison of CCE and DLE experiment results and simulation results.

2.3.4. Model construction and history matching

The reservoir model was constructed to accurately represent well spacing, fault locations, structural changes and enable accurate CO₂ movement. Table 3 presents the summary of the reservoir model properties. History match covered 31 years of production and 10 years of native CO₂ injection periods that is subdivided into primary production period, continuous gas injection period and water alternating gas injection periods and decline period after CO₂ flooding. Our strategy was tuning and matching during primary production period and then checking the others. Fig. 9 shows the history match of the field oil-water-gas production rate, and pressure. Quality of history match was checked by well by well using Eq. (3) (Schlumberger, 2013), which enabled us to quickly check the quality of the match for the whole field for all time steps for different match parameters. In this equation, "S" is

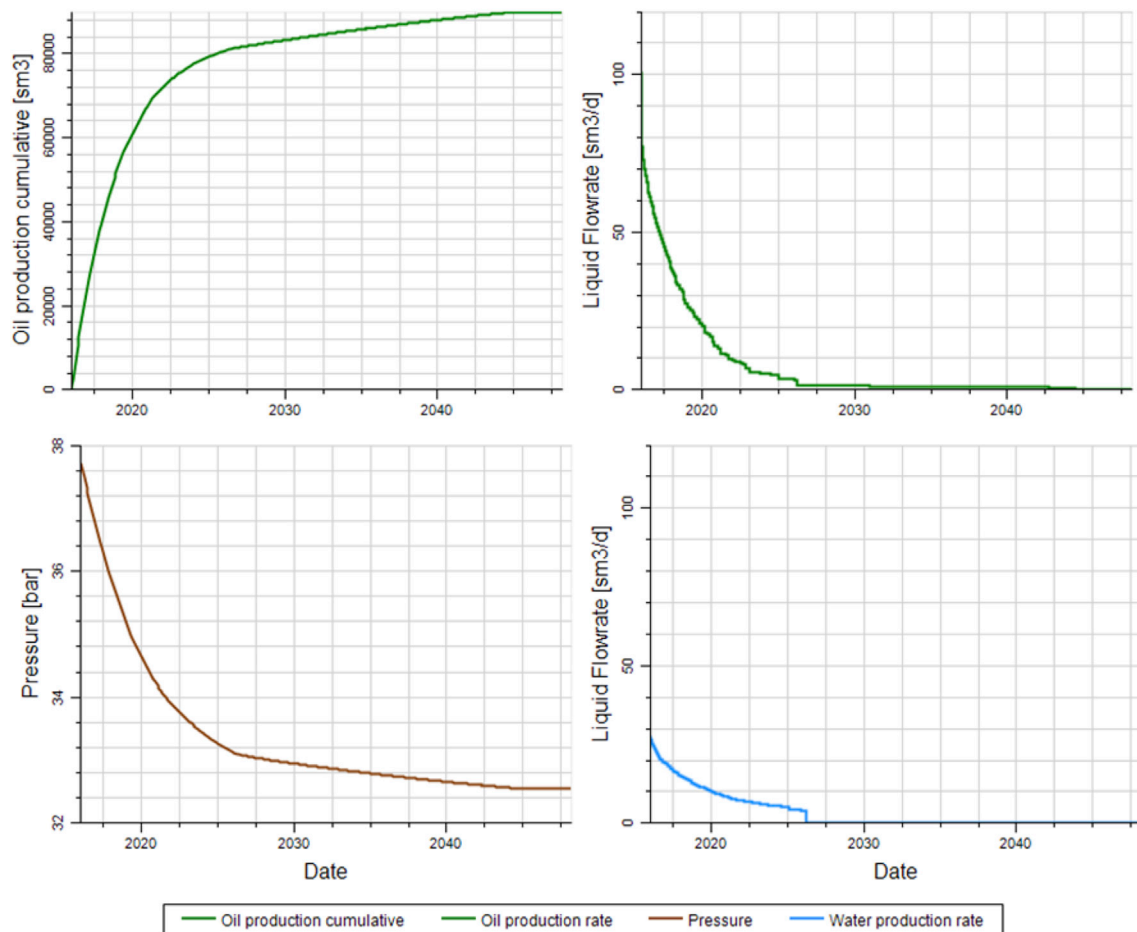


Fig. 11. Field cumulative oil production, oil rate, pressure, and water production rate for the base case.

the simulated value, “O” is the observed value, “σ” is the normalization parameter (average % observed value), “N” is the number of points and M is the match value that shows the quality of the match. Normalization parameter was used to conduct a dimensionless match in a certain range. Fig. 10 shows history match analysis of oil production rate, oil production cumulative, water cut and pressure. Most of the wells had a good match except well #3 that is located in an area with a high uncertainty.

$$M = \sqrt{\frac{1}{N} \sum_{i=1}^N \left(\frac{Si - Oi}{\sigma} \right)^2} \quad (3)$$

3. Results

Primary objective of this study is to increase the oil recovery while maximizing the flue gas storage. To achieve these goals, history matched compositional simulation model was used for numerical predictions. Sensitivity runs were carried out for different injection gas compositions, producing gas oil ratios (GOR), injection rates and CO₂ solubility. All simulation runs were started from 01.01.2016 and field production predictions for 100 years had been performed under operational constraints. For all cases, maximum water cut for production wells was set as 100% and minimum oil production for each production well was set as 0 stb/day to be able to continue the storage project in the absence of oil production. For injection wells, maximum bottom hole pressure was restrained as 131 bar that was 7 bar less than the initial reservoir pressure. A base case (do nothing case) was

run for 100 years without any gas injection for comparison purposes. Oil production had been continued for 29 years until 2045 (Fig. 11). Additional oil recovery and cumulative oil recovery was estimated as 90,000 sm³ and 1,339,721 sm³ respectively with a recovery factor of 5.7%.

In the second scenario, effect of CO₂ solubility in three phases on storage and recovery was studied. Fugacity equilibration method was used to calculate CO₂ partitioning between oil and gas (Schlumberger, 2011). Oil and gas densities and fugacity were modeled by using 3-Parameter Peng Robinson EOS. Due to lack of CO₂ solubility data in water, CO₂ solubility was determined by using solubility data from the literature (Chang et al., 1996). First run was simulated without enabling the CO₂ solubility and second run was studied enabling the CO₂ solubility in three phases. For both of the runs, GOR constraint was set as 1 000 sm³/sm³ and daily field gas injection was set as 50,000 sm³/day. Flue gas injection was started in 01.01.2016 and continued for 100 years. Fig. 12 shows oil production cumulative, gas in place, and CO₂ dissolved in aqueous phase for CO₂ solubility case and without CO₂ solubility cases. For CO₂ solubility case, cumulative flue gas storage is 1105 MMsm³, total CO₂ storage is 268 MMsm³, CO₂ dissolved in water is 19 MMsm³ and recovery factor is 10.09%. For without CO₂ solubility case, cumulative flue gas storage is 1087 MMsm³, total CO₂ storage is 262 sm³, and recovery factor is 10.06%. It was found that all of the results are very close to each other for both cases. For other scenarios, solubility option was enabled for more accurate results. Table 4 shows summary of the results of these cases.

One of the most important factors affecting amount of gas

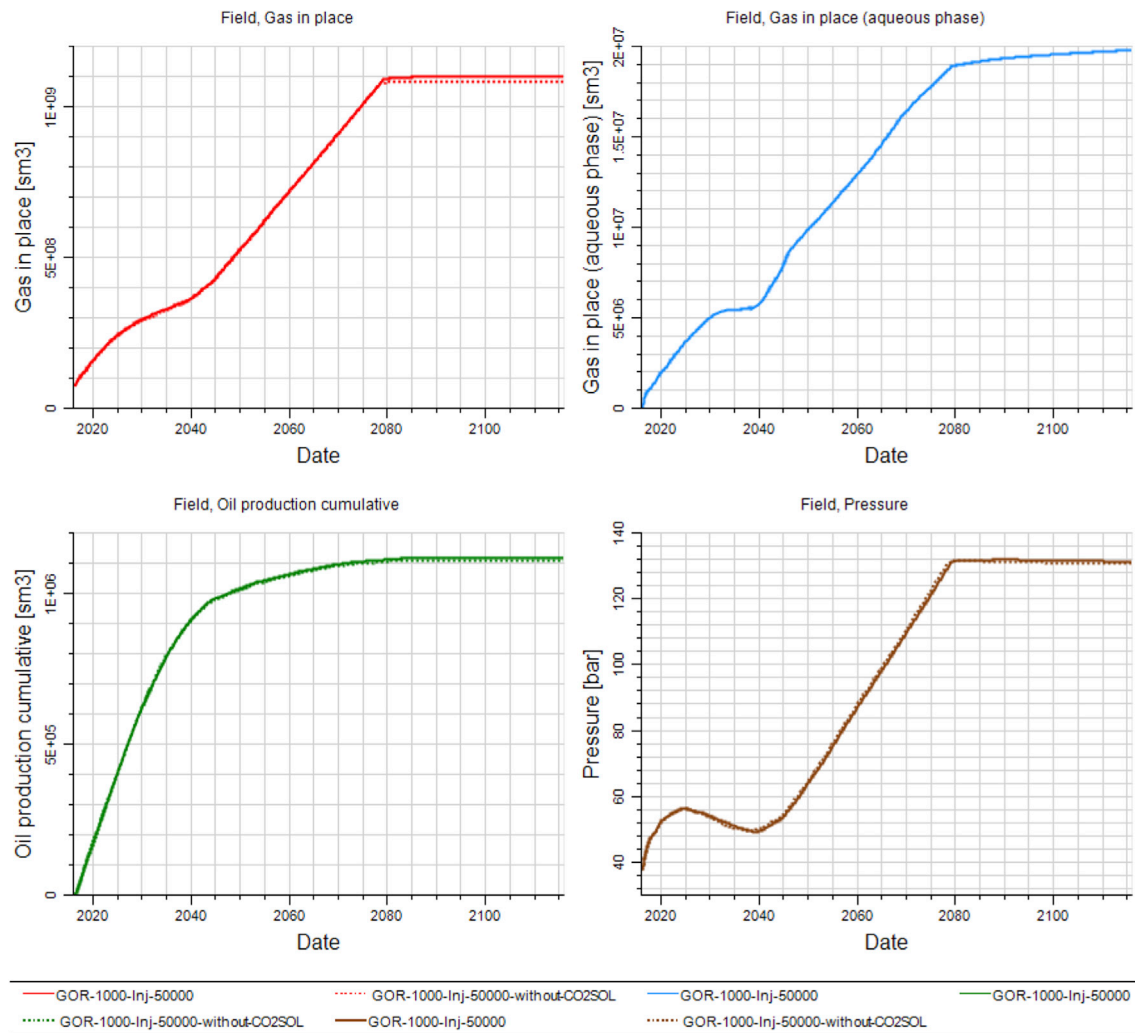


Fig. 12. Cumulative Oil Production, Gas in Place CO_2 dissolved in Aqueous Phase and Pressure with and without CO_2SOL .

sequestered is produced GOR constraint. Different GOR constraints (1, 500, 1 000 and 2000 sm^3/sm^3) were set for production wells to see the effects of GOR constraint on storage and recovery. When the simulated GOR reached the set GOR value for each well, perforations related to that increase was shut down. For all cases, daily field gas injection was set as 50,000 sm^3/day and CO_2 solubility option was enabled. Fig. 13 shows gas in place, CO_2 dissolved in aqueous phase, cumulative oil production, and average reservoir pressure for each

scenario. For very low GOR (1 sm^3/sm^3), there was almost no oil production because gas breakthrough occurred quickly in already CO_2 flooded oil field. With the closing wells due to GOR constraint, reservoir pressure increased quickly in 24 years resulting in limited increase of gas storage (Fig. 13). Better gas storage and oil recoveries were achieved in other GOR values. Maximum gas storage (1.1 billion sm^3) and improved oil recovery (10.09%) was obtained when GOR was set at 1 000 sm^3/sm^3 . Increasing GOR further (2000 sm^3/sm^3)

Table 4
Summary of the simulation results.

Case Name	Injected Gas	CO_2SOL	Flue Gas In Place, MMsm ³	CO_2 In Res, MMsm ³	CO_2 In Aqueous Phase, MMsm ³	Additional Cumulative Oil Production, sm ³	Cumulative Oil Production, sm ³	RF, %
Base Case	–	–	0.00	–	–	89,965	1,339,721	5.70
GOR-1-Inj-50000	Flue Gas	✓	642.18	190.08	10.09	715	1,250,471	5.32
GOR-500-Inj-50000	Flue Gas	✓	968.86	221.60	17.14	813,576	2,063,332	8.78
GOR-1 000-Inj-50000	Flue Gas	✓	1 105.92	268.29	19.86	1,122,280	2,372,036	10.09
GOR-1 000-Inj-50000	Flue Gas	–	1 087.26	262.52	Not Applicable	1,115,088	2,364,844	10.06
GOR-2000-Inj-50000	Flue Gas	✓	1 032.12	248.85	18.71	957,440	2,207,196	9.39
GOR-1 000-Inj-40000	Flue Gas	✓	1 088.17	260.32	18.79	1,177,198	2,426,954	10.33
GOR-1 000-Inj-75000	Flue Gas	✓	905.61	213.11	15.75	740,067	1,989,823	8.47
GOR-1 000-Inj-100000	Flue Gas	✓	853.16	197.28	14.26	615,412	1,865,168	7.94
GOR-1 000-Inj-150,000	Flue Gas	✓	843.19	195.86	14.71	598,006	1,847,763	7.86
CO_2 Injection GOR-1 000-Inj-50000	CO_2	✓	–	1 627.60	80.87	1,568,318	2,818,074	12.00

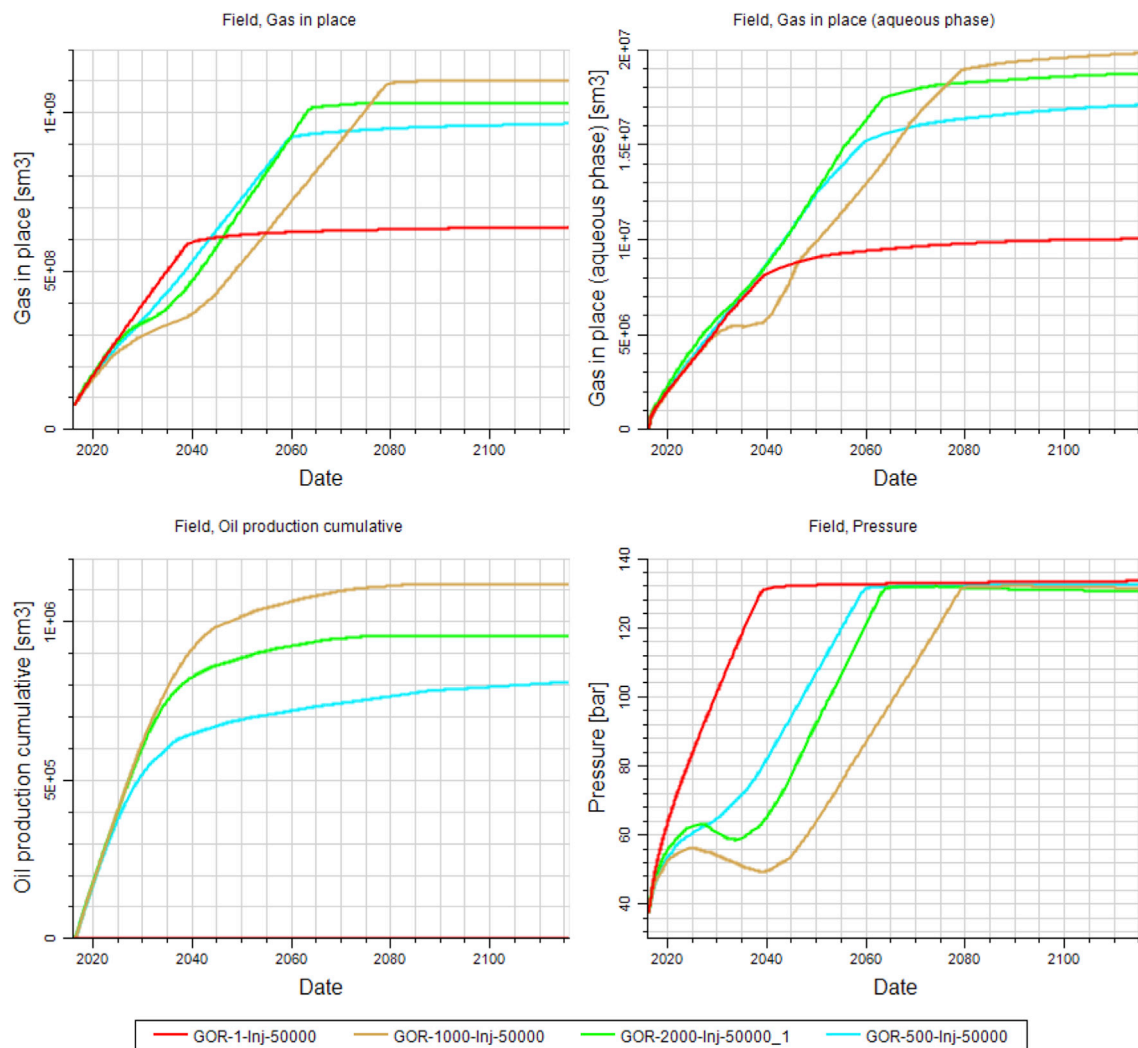


Fig. 13. Gas in Place and CO₂ dissolved in Aqueous Phase, Cumulative Oil Production, and Average Reservoir Pressure.

did not improve the gas storage and oil production. It was concluded that gas production control plays a crucial role not only for gas storage but also for oil recovery. GOR management contributes to better sweep efficiency. Moreover, oil production decreases after gas breakthrough due to high mobility of gas. Results (Table 4) showed that there is an optimum value for GOR, which maximize the amount of gas storage.

Optimization of injection rates is carried out to maximize the storage capacity of the reservoir and to increase the oil recovery. For all cases, GOR constraint was set as 1 000 sm³/sm³ and CO₂ solubility option was enabled. Simulation time, 100 years, was adjusted to determine the maximum storage capacity of the reservoir before exceeding the regulated pressure for all cases. Injection rate for each well was regulated by the bottom hole pressure constraint of 131 bars, which was 95% of the initial reservoir pressure. Maximum flue gas storage of 1.1 billion sm³ and additional oil recovery of 1.12 MMsm³ was achieved by 50,000 sm³ of daily flue gas injection and maximum oil recovery of 1.17 MMsm³ was reached by 40,000 sm³ of daily flue gas injection (Table 4). Storage capacity and oil recovery decreased as the injection rate increased. Higher injection rates caused quick pressure buildup in the reservoir resulting in limited storage capacity (Fig. 14). In addition to these, high gas injection rates resulted in early gas breakthrough so that increased the gas oil ratios which reduce the oil recovery in long term.

Finally, continuous CO₂ injection was performed instead of flue gas. Producing GOR was set as 1 000 sm³/sm³ and field gas injection rate was set as 50,000 sm³/day. Fig. 15 shows the results of the all cases and red line represents the CO₂ injection case. As can be seen from Fig. 15, CO₂ flooding trend is very different when compared with flue gas injection cases. Highest gas storage and oil recovery was achieved by CO₂ injection case. Gas storage and oil recovery continued to increase after 100 years. Totally, 1.63 billion sm³ of CO₂ was stored and 1.57 MMsm³ of oil was produced during CO₂ flooding. Fig. 16 shows the amount of flue gas storage vs recovery factor for all cases.

4. Discussion

The results of the full-field compositional simulation have been used for an examination of the raw flue gas injection, CO₂ injection, operating parameters and CO₂ solubility. Maximum CO₂ storage and oil recovery can be achieved by pure CO₂ flooding due to solubility trapping mechanism, which becomes dominant with increased CO₂ concentration and pressure. CO₂ flooding and flue gas flooding give same oil recovery for a certain time or until a certain reservoir pressure. After that, effects of CO₂ on oil lift its effectiveness. These effects are oil swelling, viscosity reduction and interfacial tension reduction due to increased CO₂ solubility. Also effect of CO₂

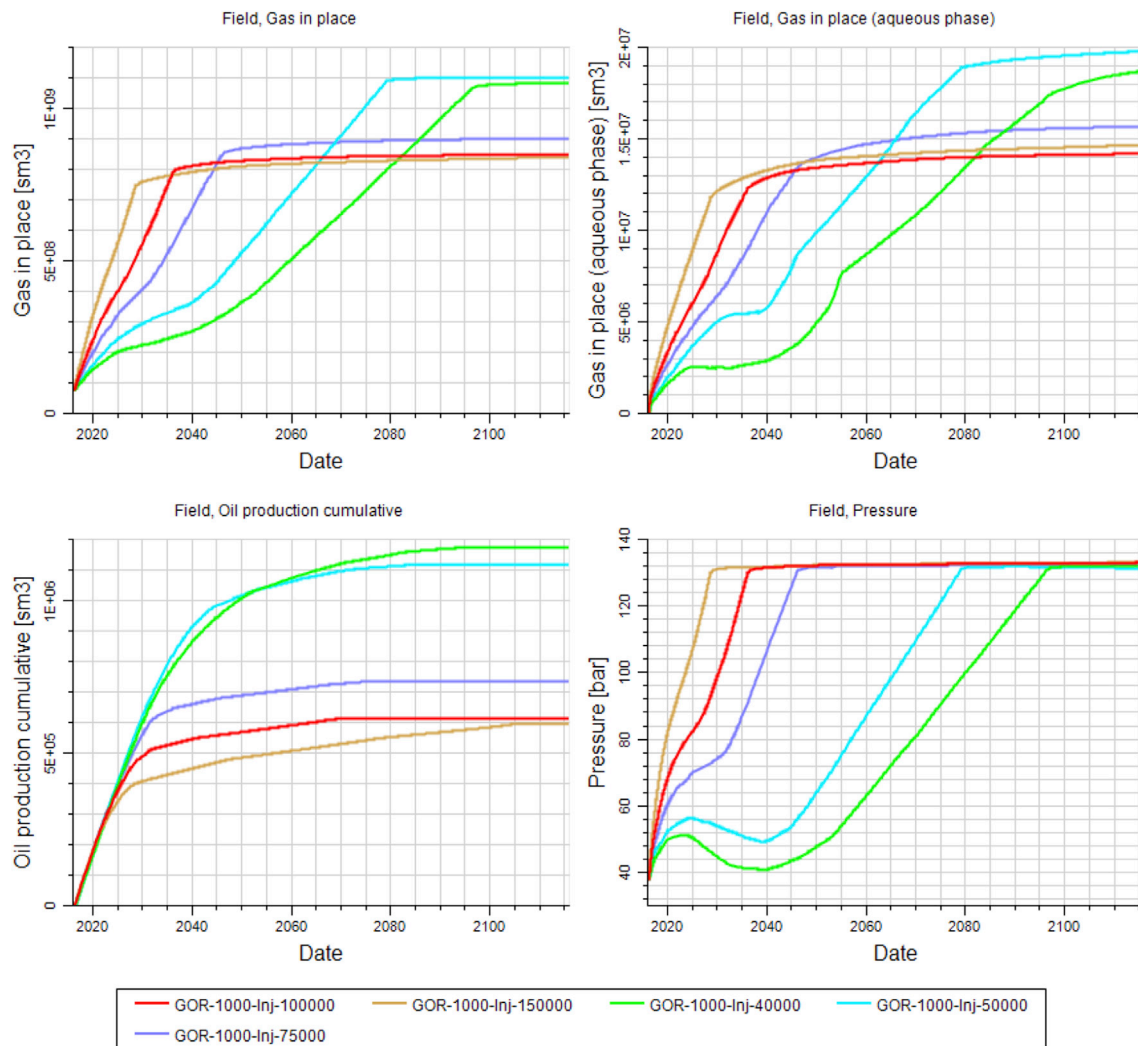


Fig. 14. Gas in Place and CO₂ dissolved in Aqueous Phase, Cumulative Oil Production, and Average Reservoir Pressure.

solubility becomes very important after this threshold time. Gas in aqueous phase (Fig. 15) shows that CO₂ dissolved in aqueous phase increases continuously corresponding to high amount of CO₂ storage. Influence of CO₂ solubility during immiscible flue gas injection is very low due to presence of impurities but it is very important during pure CO₂ injection. For mature oil reservoirs, pressurizing the reservoir with the flue gas and then injecting CO₂ might give better oil recoveries. In this way, N₂ in flue gas will provide energy to push the oil and CO₂ will dissolve in oil. In addition to these, it has been observed that water production decreases during the pressurization by gas injection. Pressure of the oil production layer increases and becomes more than the underlying layer's, which is the source of the water.

Highest oil recovery and gas storage can be achieved with optimized operating constraints targeting the sweep efficiency. With the increase in sweep efficiency, reservoir gas storage capacity and oil recovery will increase. Lower GOR values lead to quick pressure increase that decreases the project life, oil recovery and amount of CO₂ storage. On the other hand, higher GOR values give rise to gas production that in turn decrease oil recovery and gas storage with increased gas mobility and decreased sweep efficiency. High gas injection rates cause reduced injectivity due to quick pressure buildup that leads to early gas breakthrough. Both of these may cause reduction of both oil recovery and storage.

5. Conclusions

Flue gas injection in a mature oil field located in Turkey where CO₂ EOR had been applied between 2003 and 2012 was studied using a history matched compositional numerical model. Due to the availability of nearby flue gas source (cement factory) and a pipeline for gas transportation, which was built to transport natural gas from the oil field to cement factory, there is a huge opportunity to decrease project costs. A comparative study was conducted to examine the efficiency of flue gas injection compared to CO₂ injection for simultaneous EOR and storage purposes. Results showed that

1. Pure CO₂ injection leads to higher oil recovery and CO₂ storage, if injection continued for at least 25 years. Before this threshold injection time, flue gas injection and pure CO₂ injection resulted in comparable oil recoveries.
2. Amount of flue gas storage was determined as 1.1 billion sm³ and 268 MMsm³ of this gas was CO₂. Additional cumulative oil production was calculated as 1.12 MMsm³ with a recovery factor of 10.09%. 1 000 sm³ of flue gas was injected to produce 1 sm³ of oil.
3. Totally 1.63 billion sm³ of CO₂ was sequestered and 1.57 MMsm³ of oil was produced with continuous pure CO₂ flooding. 1 040 sm³ of CO₂ was injected to produce 1 sm³ of oil.

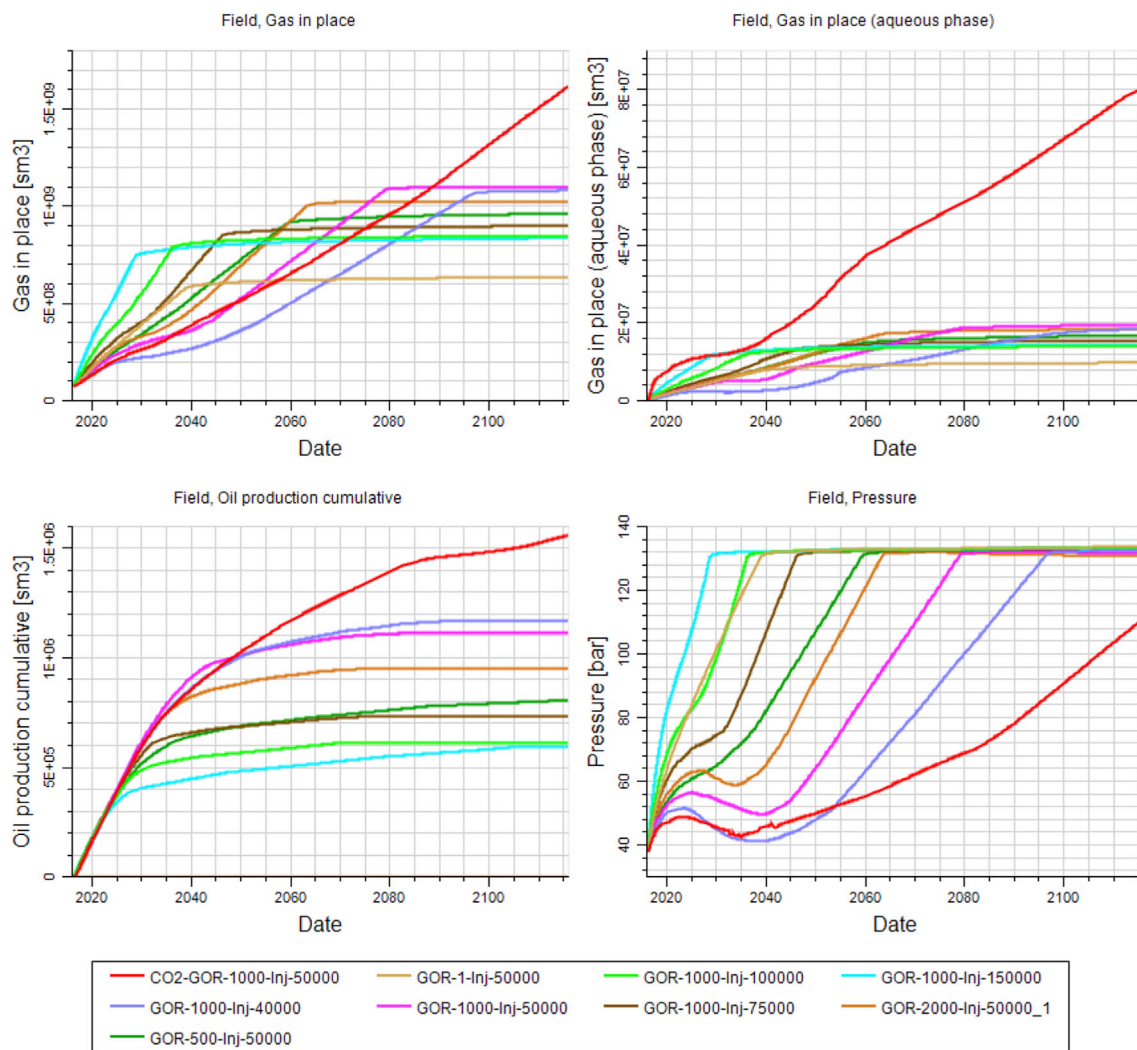


Fig. 15. Gas in Place and CO₂ dissolved in Aqueous Phase, Cumulative Oil Production, and Average Reservoir Pressure.

- Pressurizing the reservoir with flue gas injection followed by pure CO₂ injection may improve the project economics. However, pure CO₂ injection is the right strategy to maximize the CO₂ storage.
- Gas storage and oil recovery achieved with and without CO₂ solubility were very close to each other for flue gas injection due to impurities in gas.
- Limiting the production wells with lower GOR constraint, caused the wells shut down due to quick breakthrough and increased reservoir pressure suddenly which lead to diminished storage and oil recovery. Also, higher GOR values were resulted in low storage and recovery due to high gas mobility when compared with oil. Management of

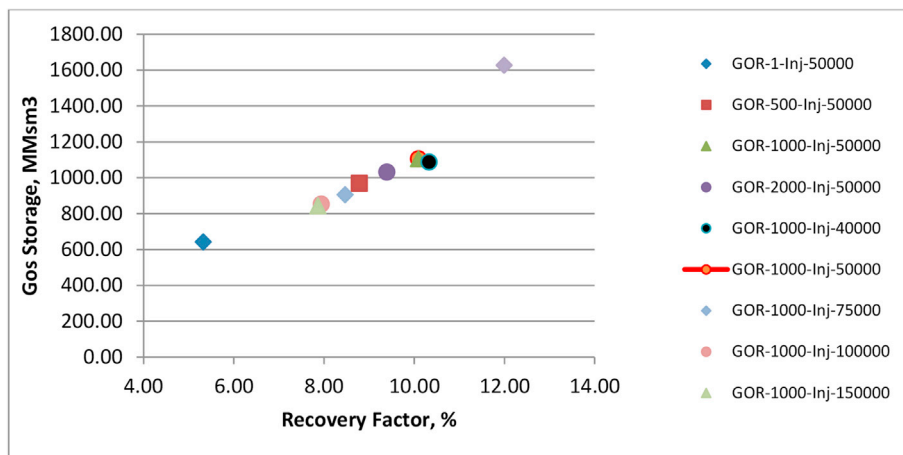


Fig. 16. Amount of Flue Gas Storage vs Recovery Factor for All Cases.

GOR values contributed to better sweep efficiency and better pressure management.

7. Injection rates need to be optimized to maximize the flue gas storage. Quick pressure buildup occurred with higher injection rates so that gas storage was reduced due to decreased injectivity. With higher injection rates, higher oil recoveries achieved at early times of the project.

Acknowledgements

The first author acknowledges scholarship support provided by the Scientific and Technological Research Council of Turkey (TUBITAK 2211-D).

References

- Al-Meshari, A.A., McCain, W.D., 2005, January 1. New Strategic Method to Tune Equation-of-state for Compositional Simulation. Society of Petroleum Engineers. <http://dx.doi.org/10.2118/106332-MS>.
- Arachchige, Udara Sampath P., Kawan, Dinsesh, Tokheim, Lars Andre, Melaaen, Morten Christian, 2013. Model development for CO₂ capture in the cement industry. *Int. J. Model. Optim.* 3 (6).
- Beckwith, R., 2011, May 1. Carbon Capture and Storage: a Mixed Review. Society of Petroleum Engineers. <http://dx.doi.org/10.2118/0511-0042-JPT>.
- Bender, S., 2011. Co-optimization of CO₂ Sequestration and Enhanced Oil Recovery and Co-optimization of CO₂ Sequestration and Methane Recovery in Geopressured Aquifers. MS thesis. University of Texas at Austin, Austin, Texas. August 2011. <http://repositories.lib.utexas.edu/bitstream/handle/2152/ETD-UT-2011-08-3771/BENDER-THESIS.pdf?sequence=1>.
- Bender, S., Yilmaz, M., 2014, April 12. Full-field Simulation and Optimization Study of Mature IWAG Injection in a Heavy Oil Carbonate Reservoir. Society of Petroleum Engineers. <http://dx.doi.org/10.2118/169117-MS>.
- Chang, Y.-B., Coats, B.K., Nolen, J.S., 1996, January 1. A Compositional Model for CO₂ Floods Including CO₂ Solubility in Water. Society of Petroleum Engineers. <http://dx.doi.org/10.2118/35164-MS>.
- Cobanoglu, M., 2001. A Numerical Study to Evaluate the Use of WAG as an EOR Method for Oil Production Improvement at B. Kozluca Field, Turkey. Paper SPE72127 presented at the SPE Asia Pacific Improved Oil Recovery Conference, Kuala Lumpur, Malaysia, 8–9 October. <http://dx.doi.org/10.2118/72127-MS>.
- Dong, M., Huang, S., 2002, September 1. Flue Gas Injection for Heavy Oil Recovery. Petroleum Society of Canada. <http://dx.doi.org/10.2118/02-09-04>.
- Eide, O., Ersland, G., Brattekas, B., Haugen, A., Graue, A., Ferno, M.A., 2015, February 1. CO₂ EOR by Diffusive Mixing in Fractured Reservoirs. Society of Petrophysicists and Well-Log Analysts.
- Fong, W.S., Tang, R.W., Emanuel, A.S., Sabat, P.J., Lambert, D.A., 1992, January 1. EOR for California Diatomites: CO₂, Flue Gas and Water Corefloods, and Computer Simulations. Society of Petroleum Engineers. <http://dx.doi.org/10.2118/24039-MS>.
- Gibbs, Michael J., Soyka, Peter, Conneely, David, Kruger, Dina, 2001. CO₂ Emissions from Cement Production. IPCC, pp. 175–182. Web.
- Huang, S.S., 1997, January 1. Comparative Effectiveness of CO₂, Produced Gas, and Flue Gas for Enhanced Heavy Oil Recovery. Society of Petroleum Engineers. <http://dx.doi.org/10.2118/37558-MS>.
- Jessen, K., Stenby, E.H., 2007, October 1. Fluid Characterization for Miscible EOR Projects and CO₂ Sequestration. Society of Petroleum Engineers. <http://dx.doi.org/10.2118/97192-PA>.
- Khan, S.A., Pope, G.A., Sepehrnoori, K., 1992, January 1. Fluid Characterization of Three-phase CO₂/Oil Mixtures. Society of Petroleum Engineers. <http://dx.doi.org/10.2118/24130-MS>.
- Koch, H.A., Hutchinson, C.A., 1958, January 1. Miscible Displacements of Reservoir Oil Using Flue Gas. Society of Petroleum Engineers.
- Kovscek, A.R., 2002. Screening criteria for CO₂ storage in oil reservoirs. *Petroleum Sci. Technol.* 20 (7&8), 841–866.
- Mahasanen, N., Dahowski, R.T., Davidson, C.L., 2005. The Role of Carbon Dioxide Capture and Storage in Reducing Emissions from Cement Plants in North America. Pacific Northwest national laboratory, 902 battelle blvd, Richland, USA.
- Marceau, Medgar L., Nisbet, Michael A., VanGeem, Martha G., 2006. Life Cycle Inventory of Portland Cement Manufacture, SN2095b. Portland Cement Association, Skokie, IL, p. 69.
- Mardin Cement. (2015). Retrieved from <http://www.mardincimento.com.tr/en/aboutus/about-mardin-cement> (Accessed 17 June 2016).
- Nazmul, H.S.M., 2005. Techno-economic Study of CO₂ Capture Process for Cement Plants. Master thesis. University of Waterloo, Ontario, Canada.
- Peng, D.Y., Robinson, D.B., 1976. A new two-constant equation of state. *Industrial Eng. Chem. Fundam.* 15, 59–64. <http://dx.doi.org/10.1021/i160057a011>.
- Pike, R., 2006, June 1. The Chemistry of Carbon Capture and Storage. Society of Petroleum Engineers. <http://dx.doi.org/10.2118/0606-0036-JPT>.
- Rao, D.N., Hughes, R.G., 2011, June 1. Current Research and Challenges Pertaining to CO₂ Flooding and Sequestration. Society of Petroleum Engineers. <http://dx.doi.org/10.2118/0211-017-TWA>.
- Reichl, A., Schneider, G., Schliepdiel, T., Reimuth, O., 2015, October 1. Carbon Capture and Storage for Enhanced Oil Recovery: Integration and Optimization of a Post-Combustion CO₂-Capture Facility at a Power Plant in Abu Dhabi. Society of Petroleum Engineers. <http://dx.doi.org/10.2118/171692-PA>.
- Rivera de la Ossa, J.E., Bejarano, A., Flórez, A., Santos, N., 2010, January 1. Experimental Evaluation of the Flue-Gas Injection of Barrancabermeja Refinery as EOR Method. Society of Petroleum Engineers. <http://dx.doi.org/10.2118/139715-MS>.
- Schlumberger, 2011. Eclipse Technical Description.
- Schlumberger, 2013. Petrel Reservoir Engineering Course.
- Shaw, J., Bachu, S., 2002, September 1. Screening, Evaluation, and Ranking of Oil Reservoirs Suitable for CO₂-Flood EOR and Carbon Dioxide Sequestration. Petroleum Society of Canada. <http://dx.doi.org/10.2118/02-09-05>.
- Shen, Lei, Gao, Tianming, Zhao, Jianan, Wang, Limao, Wang, Lan, Liu, Litao, Chen, Fengnan, Xue, Jingjing, June 2014. Factory-level measurements on CO₂ emission factors of cement production in China. *Renew. Sustain. Energy Rev.* ISSN: 1364-0321 34, 337–349. <http://dx.doi.org/10.1016/j.rser.2014.03.025>.
- Shokoya, O.S., Mehta, S.A., Moore, R.G., Maini, B.B., 2005, January 1. Effect of CO₂ Concentration on Oil Recovery in Enriched Flue Gas Flood. Petroleum Society of Canada. <http://dx.doi.org/10.2118/2005-246>.
- Testo, 2004. Flue Gas Analysis in Industry: Practical Guide for Emission and Process Measurements. Retrieved from, second ed. http://www.testo350.com/downloads/Flue_Gas_in_Industry_0981_2773.pdf (Accessed 10 June 2016).
- Trevisan, O.V., Laboissiere, P., Monte-Mor, L.S., 2013, June 11. Laboratory Study on Steam and Flue Gas Co-injection for Heavy Oil Recovery. Society of Petroleum Engineers. <http://dx.doi.org/10.2118/165523-MS>.
- Whitson, C.H., 1983. Characterizing hydrocarbon plus fractions. *SPEJ* 23 (No. 4), 683–694.
- Wickramathilaka, S., Willis, T., 2011, June 1. Carbon Capture and Sequestration: a Potential “Win-win” for the Oil Industry and the Public. Society of Petroleum Engineers. <http://dx.doi.org/10.2118/0211-020-TWA>.
- Zhang, D.X., Song, J., 2014. Mechanisms for geological carbon sequestration. *Proc. IUTAM* 10, 319–327.
- Zhang, Y.P., Sayegh, S.G., Huang, S., Dong, M., 2006, February 1. Laboratory Investigation of Enhanced Light-oil Recovery by CO/Flue Gas Huff-n-puff Process. Petroleum Society of Canada. <http://dx.doi.org/10.2118/06-02-01>.